Quasi-elastic electron scattering and nuclear shell structure

Autor(en): **Viollier, Raoul D. / Alder, Kurt**

Objekttyp: **Article**

Zeitschrift: **Helvetica Physica Acta**

Band (Jahr): **44 (1971)**

Heft 1

PDF erstellt am: **12.07.2024**

Persistenter Link: https://doi.org/10.5169/seals-114267

Quasi-Elastic Electron Scattering and Nuclear Shell Structure

by **Raoul D. Viollier** and **Kurt Alder**

Institute for Theoretical Physics, University of Basel

(20. VII. 70)

Abstract. Quasi-elastic electron scattering, knocking out a proton from the target nucleus, is treated in a distorted wave Born approximation. The coincidence cross section for the $N(e, e' p)\, N'$ reaction is calculated in the impulse approximation. Since the energy of the emitted proton depends upon the shell and its binding energy, the nuclear shell structure can be studied directly if the angular correlation of the emerging particles is measured. The angular distribution of the outgoing proton is calculated and compared with plane wave Born approximation values for ^{40}Ca, ^{32}S and ^{28}Si.

I. Introduction

The excitation of nuclear states by inelastic electron scattering has been a very useful method of investigating electromagnetic properties of nuclei. However, one obtains considerably more information about detailed nuclear structure from disintegration processes such as $N(e, e' p)\, N'$ by measuring the emerging particles in coincidence (Fig. 1a). In such an experiment we gain essentially information about the matrix element of nuclear transition current density $\langle N' p \,|\, J_\mu(x) \,|\, N \rangle$ which can be approximated by nuclear models and compared with the experiment. According to the energy transferred to the nucleus during the disintegration process $N(e, e' p)\, N'$, two cases can be distinguished: If the electron transfers a small amount of energy $\omega \ll q^2/2\, M$ (q = momentum transfer, M = nucleon mass) to the nucleus, the nucleus is excited to some intermediate state N^* which decays into the ground state by nucleon emission (Fig. 1b). In this case we gain some information about the intermediate state N^* which is essentially independent of the excitation method.

We are concerned with the opposite limit in which the electron transfers an energy $\omega \approx q^2/2\, M$ to the nucleus (Fig. 1c). In this case the nucleon is considered to be directly knocked out by the electron. By measuring the angular correlation of the emerging particles we can learn something about binding energies, nuclear shell structure and lifetimes of nuclear hole states.

Similar considerations apply to $N(p, 2p)\, N'$ experiments. However, the reaction $N(e, e' p)\, N'$ has the advantage that, since the electromagnetic interaction is well known, the excitation mechanism can be separated from nuclear structure effects and the electrons penetrate more deeply the inner nuclear shells.

Jacob and Maris [1] have published an excellent review article summarizing the theoretical and experimental work on quasi-elastic scattering of protons and electrons.

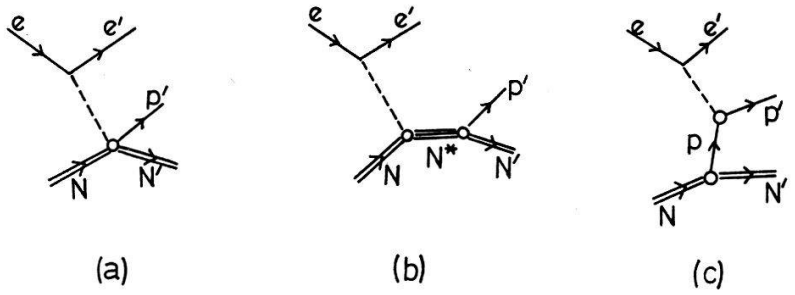

Figure 1
Disintegration process $N(e, e' p)N'$: a) without assumptions about nuclear vertex, b) the nucleus excited to some intermediate state N^* which decays by nucleon emission, c) quasi-elastic scattering.

The $N(e, e' p) N'$ reaction has been studied experimentally by Amaldi et al. [12]. In the past their experiments have been confined primarily to the determination of the binding energies of the proton in the various shells. However, they propose to conduct angular distribution studies in the near future. Such experiments give more information about nuclear shell structure since they provide a test for shell model wave functions.

Many theoretical treatments and calculations have been published. Devanathan [2] and de Forest [3] have deduced the coincidence cross section in the plane wave Born approximation (PWBA), whereas Jacob and Maris [4] and Potter [5] have calculated their cross sections by introducing the free-proton cross section in their formula.

For an exact treatment of quasi-elastic electron scattering we have to take into account the distortion of electron and proton wave functions. In the present treatment, we outline a general method for the evaluation of the coincidence cross section in a distorted wave Born approximation (DWBA). We calculate some angular distributions of the emitted proton using harmonic oscillator wave functions for the bound nucleon and compare the DWBA results for ^{40}Ca, ^{32}S and ^{28}Si with PWBA values.

In Section II the coincidence cross section for the reaction $N(e, e' p) N'$ is calculated in the DWBA for an arbitrary transition current density, which we evaluate in Section III for the case of quasi-elastic scattering. The derivation of the cross section in PWBA is given in Section IV and the numerical results are presented and discussed in Section V.

II. Evaluation of Coincidence Cross Section in DWBA

II.1. *Approximations*

Before deriving an explicit formula for the coincidence cross section for quasi-elastic electron scattering in the DWBA formalism, let us first discuss the approximations applied.

In DWBA the static electromagnetic interaction is treated exactly by solving Dirac's equation for an electron in a central field $V_0(r)$. It is assumed that the charge

distributions of the nuclear ground and excited states can be approximated by a spherically symmetric charge distribution. However, the residual interaction which is assumed to be small is treated in first order perturbation theory. This corresponds to the exchange of one photon between electron and nucleus. Since DWBA is applicable to intermediate and heavy nuclei the recoil of the nucleus can be neglected.

If the impulse approximation is valid, the proton can be considered to be knocked out directly by the electron and the many body problem is reduced essentially to a special three body problem consisting of electron, proton and residual nucleus. The inelastic electron scattering can thus be treated as quasi-elastic scattering from a single proton without excitation of the residual nucleus.

The nucleus is described by the independent particle model and it is assumed that the nucleons interact only by an average spherically symmetric potential. Therefore we confine ourselves to nuclei with closed shells or subshells.

II.2. *Formalism of DWBA*

Let us deduce the coincidence cross section for the quasi-elastic electron scattering in the DWBA formalism. The cross section for the scattering of an electron with momentum $\boldsymbol{k}_i$ to a final state $\boldsymbol{k}_f$, simultaneously knocking out a proton with momentum $\boldsymbol{p}_f$, is in first order perturbation theory given by

$$d\sigma = 2\pi\,\delta\,(W - W')\,\overline{\sum_i}\sum_f |\langle f\,|H|\,i\rangle|^2 \frac{E_i}{k_i}\,\frac{d^3\boldsymbol{k}_f}{(2\pi)^3}\,\frac{d^3\boldsymbol{p}_f}{(2\pi)^3}\,. \tag{2.1}$$

The relation of the proton momentum $\boldsymbol{p}_f$ to the electron momenta $\boldsymbol{k}_i$ and $\boldsymbol{k}_f$ is shown in Figure 2. W and W' are the total energies of the initial and final states and $\overline{\sum_i}$ denotes the average over the initial states. The electromagnetic interaction can be described by the Hamilton operator

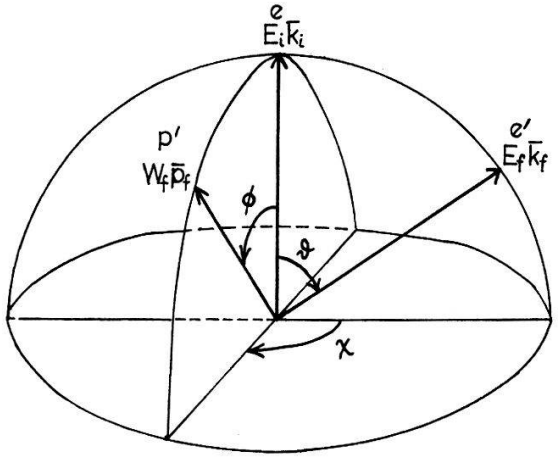

Figure 2

Relation of the momentum of an emitted proton $\boldsymbol{p}_f$ to the initial and final momenta of the electron $\boldsymbol{k}_i$ and $\boldsymbol{k}_f$.

$$H = \alpha \int d^3\boldsymbol{r}\, j_\nu(\boldsymbol{r})\, A_\nu(\boldsymbol{r}) \tag{2.2}$$

where α is the fine structure constant, $j_\nu(\boldsymbol{r})$ the transition current density of the electron

and the vector potential $A_\nu(\boldsymbol{r})$ is given by an integral over the phenomenological nuclear transition current density $\langle N' \not{p} \mid J_\nu(\boldsymbol{r}) \mid N \rangle$

$$A_\nu(\boldsymbol{r}) = \int d^3 \boldsymbol{r}' \, \langle N' \not{p} \mid J_\nu(\boldsymbol{r}') \mid N \rangle \frac{e^{i\omega \mid \boldsymbol{r}-\boldsymbol{r}' \mid}}{\mid \boldsymbol{r} - \boldsymbol{r}' \mid} \tag{2.3}$$

with

$$\omega = E_i - E_f \,. \tag{2.4}$$

The nuclear transition current density and Green's function are expandable into multipoles

$$\begin{cases} \langle N' \not{p} \mid \varrho(\boldsymbol{r}) \mid N \rangle = \sum\limits_{\lambda\mu} \varrho_{\lambda\mu}(r) \; Y^*_{\lambda\mu}(\hat{\boldsymbol{r}}) \\ \langle N' \not{p} \mid \boldsymbol{J}(\boldsymbol{r}) \mid N \rangle = -i \sum\limits_{I\lambda M} I_{I\lambda M}(r) \; \boldsymbol{Y}^*_{I\lambda M}(\hat{\boldsymbol{r}}) \end{cases} \tag{2.5}$$

and

$$\frac{e^{i\omega \mid \boldsymbol{r}-\boldsymbol{r}' \mid}}{\mid \boldsymbol{r} - \boldsymbol{r}' \mid} = 4\pi i \omega \sum_{\lambda\mu} j_\lambda(\omega r_<) \, h^{(1)}_\lambda(\omega r_>) \, Y^*_{\lambda\mu}(\hat{\boldsymbol{r}}) Y_{\lambda\mu}(\hat{\boldsymbol{r}}') \quad , \tag{2.6}$$

where

$$r_< = \min(r, r')$$
$$r_> = \max(r, r')$$

and $j_\lambda(x)$ are the spherical Bessel functions, $h^{(1)}_\lambda(x)$ the spherical Hankel functions of the first kind and $\boldsymbol{Y}_{I\lambda M}(\hat{\boldsymbol{r}})$ the vector spherical harmonics [6]. Combining equations (2.3), (2.5) and (2.6), we can write down a multipole expansion for the scalar and the vector potential, $\boldsymbol{\Phi}(\boldsymbol{r})$ and $\boldsymbol{A}(\boldsymbol{r})$, as well

$$\begin{cases} \boldsymbol{\Phi}(\boldsymbol{r}) = 4\pi i \omega \sum\limits_{\lambda\mu} \boldsymbol{\Phi}_{\lambda\mu}(r) \; Y^*_{\lambda\mu}(\hat{\boldsymbol{r}}) \\ \boldsymbol{A}(\boldsymbol{r}) = 4\pi i \omega (-i) \sum\limits_{I\lambda M} A_{I\lambda M}(r) \; \boldsymbol{Y}^*_{I\lambda M}(\hat{\boldsymbol{r}}) \,. \end{cases} \tag{2.7}$$

In equation (2.7) we have introduced the cutoff functions or the transition potentials for the different multipole orders

$$\begin{cases} \boldsymbol{\Phi}_{\lambda\mu}(r) = h^{(1)}_\lambda(\omega r) \int\limits_0^r j_\lambda(\omega r') \, \varrho_{\lambda\mu}(r') \, r'^2 \, dr' + j_\lambda(\omega r) \int\limits_r^\infty h^{(1)}_\lambda(\omega r') \, \varrho_{\lambda\mu}(r') r'^2 \, dr' \\ \\ A_{I\lambda M}(r) = h^{(1)}_I(\omega r) \int\limits_0^r j_I(\omega r') \, I_{I\lambda M}(r') \, r'^2 \, dr' + j_I(\omega r) \int\limits_r^\infty h^{(1)}_I(\omega r') \, I_{I\lambda M}(r') \, r'^2 \, dr' \,. \end{cases} \tag{2.8}$$

We can gauge the potentials $\boldsymbol{\Phi}_{\lambda\mu}(r)$ and $A_{I\lambda M}(r)$ so that the Lorentz convention and thus the equation of continuity for the nuclear current density is fulfilled

$$\begin{cases} \nabla \cdot \boldsymbol{A} + i\omega \boldsymbol{\Phi} = 0 \\ \omega \; \boldsymbol{\Phi}_{\lambda\mu}(r) + \sqrt{\dfrac{\lambda+1}{2\lambda+1}} \left(\dfrac{d}{dr} + \dfrac{\lambda+2}{r} \right) A_{\lambda\,\lambda+1\,\mu}(r) - \\ \qquad - \sqrt{\dfrac{\lambda}{2\lambda+1}} \left(\dfrac{d}{dr} - \dfrac{\lambda-1}{r} \right) A_{\lambda\,\lambda-1\,\mu}(r) = 0 \,. \end{cases} \tag{2.9}$$

The transition current density of the electron is given by (see Appendix)

$$\begin{Bmatrix} \varrho(\boldsymbol{r}) \\ \boldsymbol{j}(\boldsymbol{r}) \end{Bmatrix} = \begin{Bmatrix} \psi^+_{\tau_f}\psi_{\tau_i} \\ \psi^+_{\tau_f}\boldsymbol{\alpha}\psi_{\tau_i} \end{Bmatrix} = (4\pi)^2 \sqrt{\frac{(E_i+m)(E_f+m)}{4E_iE_f}}$$

$$\sum_{\substack{\varkappa_i\mu_i \\ \varkappa_f\mu_f}} i^{l_f-l_i}\hat{j}_f\hat{j}_i(-1)^{\mu_f+\mu_i-1}\begin{pmatrix} l_f & \frac{1}{2} & j_f \\ \mu_f-\tau_f & \tau_f-\mu_f & \end{pmatrix}\begin{pmatrix} l_i & \frac{1}{2} & j_i \\ \mu_i-\tau_i & \tau_i-\mu_i & \end{pmatrix}$$

$$Y_{l_f\mu_f-\tau_f}(\hat{\boldsymbol{k}}_f)\,Y^*_{l_i\mu_i-\tau_i}(\hat{\boldsymbol{k}}_i)\,e^{i(\delta_{\varkappa_f}+\delta_{\varkappa_i})}\begin{Bmatrix} \psi^{\mu_f}_{\varkappa_f}+\psi^{\mu_i}_{\varkappa_i} \\ \psi^{\mu_f}_{\varkappa_f}+\boldsymbol{\alpha}\psi^{\mu_i}_{\varkappa_i} \end{Bmatrix}. \tag{2.10}$$

Now we can calculate the matrix element of the Hamilton operator by the integral (2.2) (see Appendix). The formulae become particularly simple if we introduce the incident beam coordinate system. Thus the transition amplitude for a multipole transition $E\,\lambda$ or $M\,\lambda$ becomes

$$T_{\lambda\mu} = 8\pi^2\omega\alpha\sqrt{\frac{(E_i+m)(E_f+m)}{E_iE_f}}\; i(-1)^{\tau_i-1/2}(-1)^{\mu}\hat{\lambda}$$

$$\sum_{\varkappa_i\varkappa_f}\hat{j}_f^2\hat{j}_i^2\hat{l}_i\begin{pmatrix} l_f & \frac{1}{2} & j_f \\ \mu_f-\tau_f & \tau_f-\mu_f & \end{pmatrix}\begin{pmatrix} l_i & \frac{1}{2} & j_i \\ 0 & \tau_i-\tau_i & \end{pmatrix}\begin{pmatrix} j_f & \lambda & j_i \\ -\mu_f & -\mu & -\tau_i \end{pmatrix}\begin{pmatrix} j_f & \lambda & j_i \\ \frac{1}{2} & 0 & -\frac{1}{2} \end{pmatrix}$$

$$Y_{l_f\mu_f-\tau_f}(\hat{\boldsymbol{k}}_f)\,i^{l_f-l_i}\,e^{i(\delta_{\varkappa_f}+\delta_{\varkappa_i})}\{R_{\varkappa_i\varkappa_f}(E\,\lambda,\mu)+R_{\varkappa_i\varkappa_f}(M\,\lambda,\mu)\}, \tag{2.11}$$

where by reason of the parity selection rule the radial integral for an electric multipole transition $R_{\varkappa_i\varkappa_f}(E\,\lambda,\mu)$ contributes only for

$$l_i(\varkappa_i)+\lambda+l_f(\varkappa_f) = \text{even} \tag{2.12}$$

and the radial matrix element for a magnetic transition $R_{\varkappa_i\varkappa_f}(M\,\lambda,\mu)$ only for

$$l_i(\varkappa_i)+\lambda+l_f(\varkappa_f) = \text{odd}\,. \tag{2.13}$$

In (2.11) we have introduced the radial integrals

$$R_{\varkappa\varkappa'}(E\,\lambda,\mu) = \int_0^\infty r^2\,dr\Big\{(f_\varkappa f_{\varkappa'}+g_\varkappa g_{\varkappa'})\,\Phi_{\lambda\mu}(r)$$

$$-\frac{1}{\sqrt{\lambda(2\lambda+1)}}[(\varkappa'-\varkappa)(f_\varkappa g_{\varkappa'}+g_\varkappa f_{\varkappa'})-\lambda(f_\varkappa g_{\varkappa'}-g_\varkappa f_{\varkappa'})]\,A_{\lambda\lambda-1\mu}(r)$$

$$-\frac{1}{\sqrt{(\lambda+1)(2\lambda+1)}}[(\varkappa'-\varkappa)(f_\varkappa g_{\varkappa'}+g_\varkappa f_{\varkappa'})+(\lambda+1)(f_\varkappa g_{\varkappa'}-g_\varkappa f_{\varkappa'})]\,A_{\lambda\lambda+1\mu}(r)\Big\} \tag{2.14}$$

and

$$R_{\varkappa\varkappa'}(M\,\lambda,\mu) = -\int_0^\infty r^2\,dr\,\frac{\varkappa+\varkappa'}{\sqrt{\lambda(\lambda+1)}}(f_\varkappa g_{\varkappa'}+g_\varkappa f_{\varkappa'})\,A_{\lambda\lambda\mu}(r)\,. \tag{2.15}$$

Now the coincidence cross section of quasi-elastic electron scattering when the electron beam and the target nuclei are unpolarized is given by

$$\frac{d\sigma}{d\Omega_e\,d\Omega_p\,dE_f} = \frac{E_i}{k_i}\,\frac{E_f\,k_f\,W_f\,p_f}{(2\pi)^5}\sum_{\tau_iM_i\sigma_f}\Big|\sum_{\lambda\mu}T_{\lambda\mu}\Big|^2 \tag{2.16}$$

with

$$W_f^2 = P_f^2 + M^2 .$$

In equation (2.16) we have averaged and summed over the unobserved quantities. The summation over τ_f can be carried out with the help of a symmetry relation.

III. Nuclear Transition Current Density

In order to evaluate the cross section of quasi-elastic electron scattering we require the matrix element of the nuclear transition current density $\langle N' p \,|\, J_\mu(x) \,|\, N\rangle$. If the impulse approximation holds, the electron is scattered by a single proton. Thus the nuclear transition charge and current densities for closed shells and subshells are given by

$$\begin{cases} \langle N' p \,|\varrho(\boldsymbol{r})|\, N\rangle = \Psi^+_{\sigma_f} \Psi^{M_i}_{K_i} \\ \langle N' p \,|\boldsymbol{J}(\boldsymbol{r})|\, N\rangle = \Psi^+_{\sigma_f} \boldsymbol{\alpha}\, \Psi^{M_i}_{K_i} \cdot \end{cases} \tag{3.1}$$

The proton wave functions, $\Psi^{M_i}_{K_i}$ and Ψ_{σ_f}, are assumed to be solutions of Dirac's equation for a particle in a central field (see Appendix)

$$\Psi_{\sigma_f} = 4\pi \sqrt{\frac{W_f + M}{2 W_f}} \sum_{K_f M_f} e^{-i\delta_{K_f}} i^{-L_f} \hat{I}_f \begin{pmatrix} L_f & \frac{1}{2} & I_f \\ M_f - \sigma_f & \sigma_f & -M_f \end{pmatrix} (-1)^{M_f - 1/2} Y^*_{L_f M_f - \sigma_f}(\hat{\boldsymbol{p}}_f)\, \Psi^{M_f}_{K_f} \tag{3.2}$$

and the Dirac spinors are given by

$$\Psi^{M_i}_{K_i} = \begin{pmatrix} G_{K_i} \chi^{M_i}_{K_i} \\ 0 \end{pmatrix}, \quad \Psi^{M_f}_{K_f} = \begin{pmatrix} G_{K_f} \chi^{M_f}_{K_f} \\ i F_{K_f} \chi^{M_f}_{-K_f} \end{pmatrix} . \tag{3.3}$$

Let us now calculate the radial functions

$$\begin{cases} \varrho_{\lambda\mu}(r) = \int \langle N' p \,|\varrho(\boldsymbol{r})|\, N\rangle\, Y_{\lambda\mu}(\hat{\boldsymbol{r}})\, d\Omega \\ I_{I\lambda M}(r) = i \int \langle N' p \,|\boldsymbol{J}(\boldsymbol{r})|\, N\rangle\, \boldsymbol{Y}_{I\lambda M}(\hat{\boldsymbol{r}})\, d\Omega . \end{cases} \tag{3.4}$$

If we introduce the transition current density (3.2) in equations (3.4), the following integrals occur for electric $E\,\lambda$ transitions

$$\begin{aligned} &\int \Psi^{M_f +}_{K_f}\, Y_{\lambda\mu}\, \Psi^{M_i}_{K_i}\, d\Omega = G_{K_i} G_{K_f} \langle K_f M_f \,|\, Y_{\lambda\mu} \,|\, K_i M_i\rangle \\ &\int \Psi^{M_f +}_{K_f}\, \boldsymbol{\alpha}\cdot \boldsymbol{Y}_{\lambda\lambda-1\mu}\, \Psi^{M_i}_{K_i}\, d\Omega = \frac{i\,(K_f - K_i + \lambda)}{\sqrt{\lambda\,(2\lambda+1)}}\, G_{K_i} F_{K_f} \langle K_f M_f \,|\, Y_{\lambda\mu} \,|\, K_i M_i\rangle \\ &\int \Psi^{M_f +}_{K_f}\, \boldsymbol{\alpha}\cdot \boldsymbol{Y}_{\lambda\lambda+1\mu}\, \Psi^{M_i}_{K_i}\, d\Omega = \frac{i\,(K_f - K_i - \lambda - 1)}{\sqrt{(\lambda+1)\,(2\lambda+1)}}\, G_{K_i} F_{K_f} \langle K_f M_f \,|\, Y_{\lambda\mu} \,|\, K_i M_i\rangle \end{aligned} \tag{3.5}$$

and for magnetic $M\,\lambda$ transitions

$$\int \Psi^{M_f +}_{K_f}\, \boldsymbol{\alpha}\cdot \boldsymbol{Y}_{\lambda\lambda\mu}\, \Psi^{M_i}_{K_i}\, d\Omega = \frac{-i\,(K_i + K_f)}{\sqrt{\lambda\,(\lambda+1)}}\, G_{K_i} F_{K_f} \langle -K_f\, M_f \,|\, Y_{\lambda\mu} \,|\, K_i\, M_i\rangle \cdot \tag{3.6}$$

The matrix elements $\langle \pm K_f M_f | Y_{\lambda\mu} | K_i M_i \rangle$ can be expressed in terms of 3 j-symbols (see Appendix). Thus the radial functions $\varrho_{\lambda\mu}(r)$ and $I_{I\lambda M}(r)$ are given for $E\,\lambda$ transitions by

$$\begin{cases} \varrho_{\lambda\mu}(r) = \sum\limits_{K_f\,even} a_{K_f\lambda\mu}\, G_{K_f}\, G_{K_i} \\ I_{\lambda\lambda-1\mu}(r) = \sum\limits_{K_f\,even} a_{K_f\lambda\mu} \dfrac{K_i - K_f - \lambda}{\sqrt{\lambda\,(2\lambda+1)}}\, G_{K_i}\, F_{K_f} \\ I_{\lambda\lambda+1\mu}(r) = \sum\limits_{K_f\,even} a_{K_f\lambda\mu} \dfrac{K_i - K_f + \lambda + 1}{\sqrt{(\lambda+1)\,(2\lambda+1)}}\, G_{K_i}\, F_{K_f} \end{cases} \tag{3.7}$$

and for $M\,\lambda$ transitions by

$$I_{\lambda\lambda\mu}(r) = \sum_{K_f\,odd} a_{K_f\lambda\mu} \frac{K_i + K_f}{\sqrt{\lambda\,(\lambda+1)}}\, G_{K_i}\, F_{K_f} \tag{3.8}$$

where we have introduced the coefficient

$$a_{K_f\lambda\mu} = -\sqrt{4\pi}\,\sqrt{\frac{W_f + M}{2\,W_f}}\; e^{i\delta_{K_f}}\, i^{L_f} \hat{I}_f^{\,2}\, \hat{\lambda}\; \hat{I}_i \begin{pmatrix} L_f & \frac{1}{2} & I_f \\ M_f - \sigma_f & \sigma_f & -M_f \end{pmatrix}$$

$$\begin{pmatrix} I_f & \lambda & I_i \\ -M_f & \mu & M_i \end{pmatrix} \begin{pmatrix} I_f & \lambda & I_i \\ \frac{1}{2} & 0 & -\frac{1}{2} \end{pmatrix} Y_{L_f M_f - \sigma_f}(\hat{\boldsymbol{p}}_f) \quad \cdot$$

$$\sum_{K_f \left\{ \substack{even \\ odd} \right\}} \text{denotes} \sum_{K_f} \text{with } L_f(K_f) + \lambda + L_i(K_i) = \begin{Bmatrix} \text{even} \\ \text{odd} \end{Bmatrix} \cdot \tag{3.9}$$

IV. Cross Section in PWBA

In this chapter we evaluate the cross section for the quasi-elastic electron scattering in PWBA. The matrix element of the electromagnetic interaction is given by

$$\langle f | H | i \rangle = \frac{4\pi i \alpha}{q_\mu^2}\, \bar{u}^{(r')}(\boldsymbol{k}_f)\, \gamma_\mu\, u^{(r)}(\boldsymbol{k}_i)\, J_\mu \quad \cdot \tag{4.1}$$

J_μ is the Fourier integral of the nuclear transition current density

$$J_\mu = \int d^3\boldsymbol{x}\, e^{i\boldsymbol{q}\boldsymbol{x}} \langle N'\, p\, | J_\mu(\boldsymbol{x}) | N \rangle \tag{4.2}$$

and q_μ^2 the square of the momentum transfer

$$q_\mu^2 = \boldsymbol{q}^2 - \omega^2\,. \tag{4.3}$$

For the Dirac spinors we have chosen the normalization of Källén [7]. Since we do not observe a polarization of the electron we average over the initial and sum over the final states of the electron

$$\tfrac{1}{2} \sum_{rr'} |\langle f | H | i \rangle|^2 = \left(\frac{4\pi\alpha}{q_\mu^2} \right)^2 N_{\mu\nu}\, J_\mu\, \tilde{J}_\nu \quad \cdot \tag{4.4}$$

In equation (4.4) we have introduced the expressions

$$N_{\mu\nu} = \frac{1}{2 E_i E_f} (k_{i\mu} k_{f\nu} + k_{f\mu} k_{i\nu} + \frac{1}{2} q_\mu^2 \delta_{\mu\nu}) \tag{4.5}$$

and

$$J_\mu = (\boldsymbol{J}, i\varrho) , \quad \tilde{J}_\mu = (\boldsymbol{J}^*, i\varrho^*) . \tag{4.6}$$

Now let us evaluate the Fourier integral of the nuclear transition current density

$$\begin{cases} \varrho = \int \langle N' p \,|\varrho(\boldsymbol{r})|\, N\rangle e^{i\boldsymbol{q}\boldsymbol{r}} d^3\boldsymbol{r} = 4\pi \sum_{\lambda\mu} i^\lambda R_{\lambda\mu} Y^*_{\lambda\mu}(\hat{\boldsymbol{q}}) \\ \boldsymbol{J} = \int \langle N' p \,|\boldsymbol{J}(\boldsymbol{r})|\, N\rangle e^{i\boldsymbol{q}\boldsymbol{r}} d^3\boldsymbol{r} = -4\pi i \sum_{I\lambda M} i^\lambda S_{I\lambda M} Y^*_{I\lambda M}(\hat{\boldsymbol{q}}) . \end{cases} \tag{4.7}$$

The radial integrals are given by

$$\begin{cases} R_{\lambda\mu} = \int_0^\infty \varrho_{\lambda\mu}(r)\, j_\lambda(q r)\, r^2 dr \\ S_{I\lambda M} = \int_0^\infty I_{I\lambda M}(r)\, j_\lambda(q r)\, r^2 dr . \end{cases} \tag{4.8}$$

The formulae (4.7) become particularly simple if we introduce the coordinate system in which $\boldsymbol{q}$ lies in the direction of the z-axis

$$\begin{cases} \varrho = \sqrt{4\pi} \sum_\lambda i^\lambda \hat{\lambda}\, R_{\lambda 0} , \\ \boldsymbol{J} = -i\sqrt{4\pi} \sum_{I\lambda\tau} i^\lambda \langle \lambda\, 0\, 1\, \tau \,|\, I\, \tau\rangle \hat{\lambda}\, S_{I\lambda\tau} \boldsymbol{\chi}^*_\tau . \end{cases} \tag{4.9}$$

$\boldsymbol{\chi}_\tau$ are the spherical unit vectors

$$\begin{cases} \boldsymbol{\chi}_1 = -\frac{1}{\sqrt{2}} (\boldsymbol{e}_x + i\, \boldsymbol{e}_y) \\ \boldsymbol{\chi}_0 = \boldsymbol{e}_z \\ \boldsymbol{\chi}_{-1} = \frac{1}{\sqrt{2}} (\boldsymbol{e}_x - i\, \boldsymbol{e}_y) . \end{cases} \tag{4.10}$$

The average and sum over the initial and final states of the proton are simplified by application of a symmetry relation

$$\overline{\sum_i} \sum_f J_\mu \tilde{J}_\nu = \sum_{M_i \sigma_f} J_\mu \tilde{J}_\nu = 2 \sum_{M_i} J_\mu \tilde{J}_\nu . \tag{4.11}$$

Thus the coincidence cross section is given by

$$\frac{d\sigma}{d\Omega_e\, d\Omega_p\, dE_f} = \frac{E_i}{k_i} \frac{E_f k_f W_f p_f}{(2\pi)^5} \left(\frac{4\pi\alpha}{q_\mu^2}\right)^2 N_{\mu\nu} 2 \sum_{M_i} J_\mu \tilde{J}_\nu . \tag{4.12}$$

V. Numerical Results and Discussion

In this section we present some numerical results of quasi-elastic scattering of electrons from nuclei and discuss those parts of the calculation in which the numerical procedures are of interest.

The problem of calculation falls naturally into two parts: (1) The evaluation of the radial integrals and (2) the calculation of the cross section. The numerical calculation of radial integrals is accomplished by the method of Runge-Kutta-Gill.

Normalization of the wave functions and determination of the phase shifts is achieved by comparison of the calculated values $f_\varkappa$ and $g_\varkappa$ with their WKB-solutions at some large value $r = R$ (see Appendix). Once the radial integrals are known, the evaluation of the cross section is easily performed by means of equation (2.16). In order to speed the convergence of the series in equation (2.11), we made use of the reduced series as Yennie et al. [11]. This powerful method is based on the recursion relation for spherical harmonics. The reduced series converges considerably faster than the original series.

As the calculations are rather extensive a few representative examples have been selected for discussion. In the following calculations, the radial dependence of the ground state charge distribution has been taken to be of the Fermi shape:

$$\varrho(r) = \frac{\varrho_0}{1 + \dfrac{r - c}{t/4.4}} \,. \tag{5.1}$$

For the bound proton we have used harmonic oscillator wavefunctions (see Appendix), and the emitted proton has been assumed to be distorted by a square well potential of the depth V. The oscillator parameter λ is determined by finding the expectation value of the square of the nuclear radius $\langle r^2 \rangle$ (see Appendix), which is given by

$$\langle r^2 \rangle = R_0^2 \, A^{2/3}, \tag{5.2}$$

where A is the number of nucleons in the nucleus and R_0 has been fixed to $R_0 = 1.4$ F.

Numerical calculations are carried out at incident energies of 200 MeV and 300 MeV, and a study of the behaviour of the cross section is made for the closed shell and subshell nuclei ^{40}Ca, ^{32}S and ^{28}Si at a fixed electron scattering angle $\vartheta = 50^0$. It is in principle possible to distinguish the proton emitted from different shells by measuring the energy of the outgoing proton. The assumed binding energies of the proton in the various nuclear shells are given in Figure 3.

The maximum cross section is obtained for $\chi = 180^0$, when all three vectors $\boldsymbol{k}_i$, $\boldsymbol{k}_f$ and $\boldsymbol{p}_f$ are coplanar. Experimentally this is the most favorable arrangement, therefore we confine our theoretical study to this particular case.

Some typical results are presented in Figures 4–12 where we show the angular distribution of the emitted proton obtained from the exact calculation (DWBA) and the PWBA for different nuclear potential depths. The coincidence cross section for quasi-elastic scattering by a 1 $d_{5/2}$ shell proton of ^{28}Si is given in Figure 4. We have plotted the exact calculation (solid curve) and the PWBA (dashed curve) for the potential depths $V = 0$ and $V = 10$ MeV. The angular distribution of the knock-out proton shows a minimum around the proton angle $\varphi = 50^0$. The main effect of nuclear

distortion can be treated by replacing the proton momentum p_f by an effective momentum p_{eff} within the nucleus

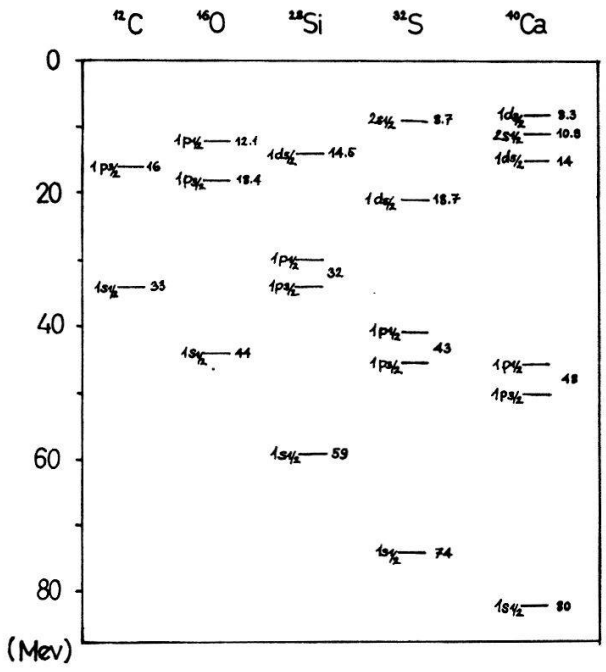

Figure 3
Binding energies of the proton assumed in the calculation.

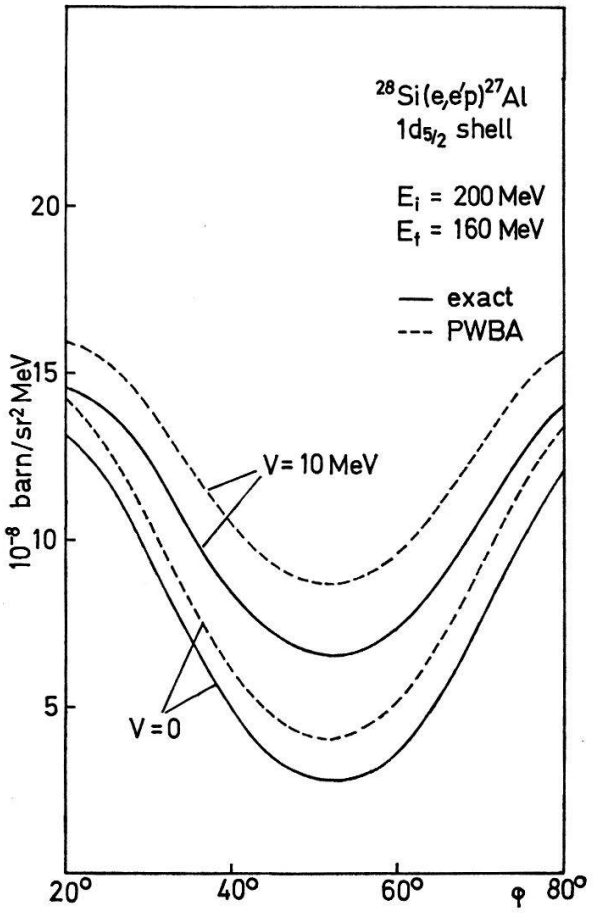

Figure 4
The coincidence cross section for the 1 $d_{5/2}$ shell of ^{28}Si at an ingoing electron energy $E_i = 200$ MeV and an outgoing electron energy $E_f = 160$ MeV. The solid curve represents the exact calculation (DWBA) and the dashed curve the PWBA. The outgoing proton has been distorted by a potential of depth $V = 0$ and $V = 10$ MeV.

$$\begin{cases} p_{eff} = \sqrt{W_{eff}^2 - M^2} \\ W_{eff} = W_f + V \end{cases} . \tag{5.3}$$

In Figures 5–7 the angular distribution of a proton emerging from the 2 $s_{1/2}$ shell of ^{32}S is given for three different electron energies. At an ingoing (outgoing) electron energy $E_i = 200$ MeV ($E_f = 160$ MeV) the angular distribution shows a peak around $\varphi = 50^0$ and two minima (Fig. 5). In contrast to Figure 4 the shape of the distribution is sensitive to the depth of the nuclear potential V. The curves with $V = 0$ show very pronounced peaks, whereas the curves with $V = 10$ MeV are washed out.

By varying the electron energies the behaviour of the angular distribution is completely changed due to the different effective momentum p_{eff}. At $E_i = 300$ MeV and $E_f = 220$ MeV the angular correlation shows only one peak for $V = 19$ MeV, but

if the nuclear distortion is neglected a double peaking appears (Fig. 6). At $E_f =$ 230 MeV this double peaking is very much pronounced for $V = 0$ and can be seen even if the outgoing proton wave function is distorted by a nuclear potential of the depth $V = 19$ MeV (Fig. 7).

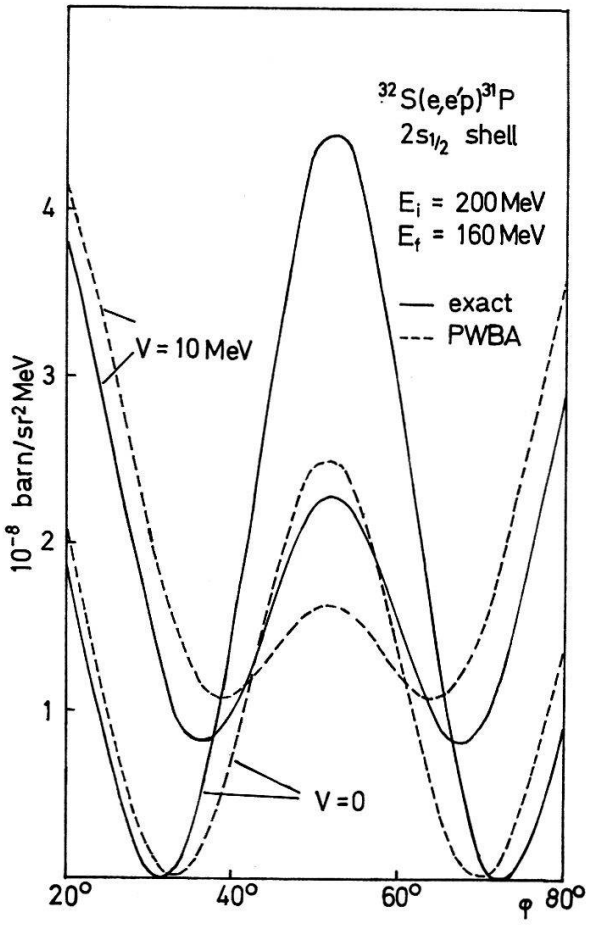

Figure 5
The coincidence cross section for the 2 $s_{1/2}$ shell of ^{32}S. $E_i = 200$ MeV, $E_f = 160$ MeV, potential depths $V = 0$ and $V = 10$ MeV.

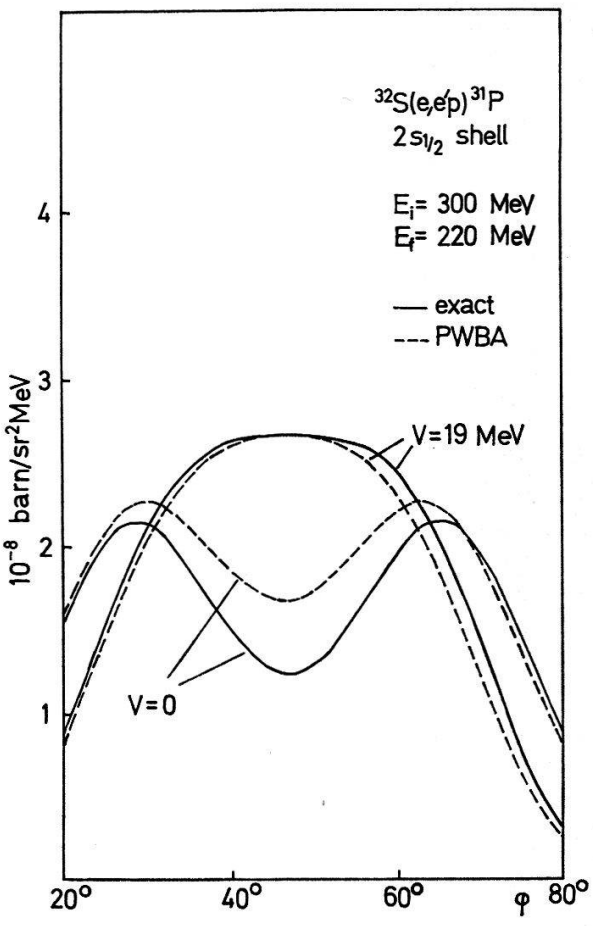

Figure 6
The coincidence cross section for the 2 $s_{1/2}$ shell of ^{32}S. $E_i = 300$ MeV, $E_f = 220$ MeV, potential depths $V = 0$ and $V = 19$ MeV.

The angular distribution of the outgoing proton knocked out from the 1 $d_{5/2}$ shell of ^{32}S for $E_i = 300$ MeV is given in Figures 8 and 9. As in the case of the 2 $s_{1/2}$ shell we have a maximum around $\varphi = 50^0$ for $V = 23$ MeV and $E_f = 220$ MeV (Fig. 8). For $V = 0$ the effective proton momentum p_{eff} is lower and the double peaking appears again in our curve. The same happens if we change the outgoing electron energy to $E_f = 230$ MeV (Fig. 9). This gives us a weak minimum around $\varphi = 50^0$ for $V = 23$ MeV and two very pronounced peaks in the case of $V = 0$.

For discussion of the 1 $d_{3/2}$ shell we have selected the nucleus ^{40}Ca. In Figures 10–12 the angular distribution of the 1 $d_{3/2}$ shell proton of ^{40}Ca is shown at different electron energies. The shapes of the angular correlations are similar to those of the 1 $d_{5/2}$ shells. The main difference lies in the binding energies of the bound proton. The binding energy of a 1 $d_{3/2}$ shell proton in ^{40}Ca ($B = 8.3$ MeV) is much smaller than the binding energy of a 1 $d_{5/2}$ shell proton in ^{32}S ($B = 18.7$ MeV). This affects the effective momentum p_{eff} and therefore the double peaking appears only weakly in Figures 10 and 12.

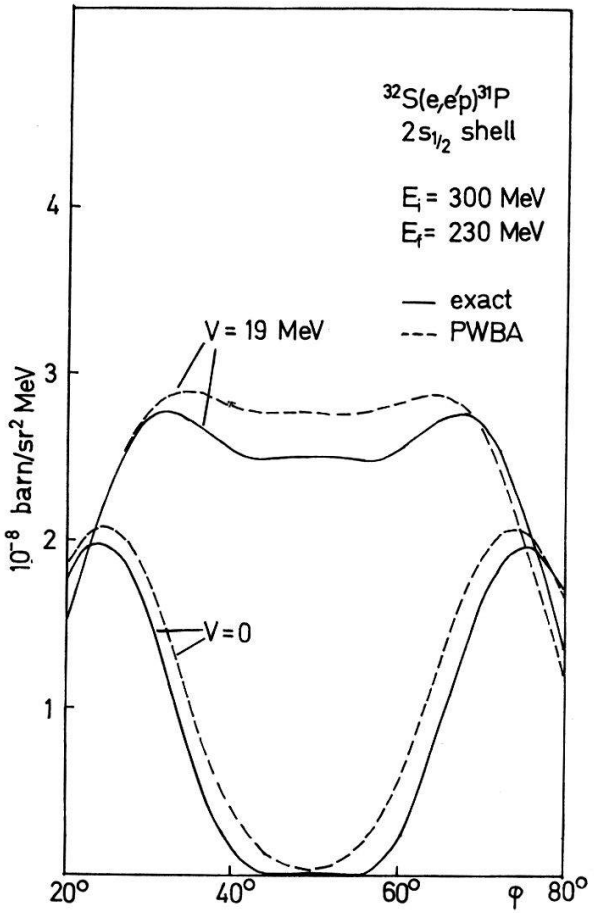

Figure 7

The coincidence cross section for the 2 $s_{1/2}$ shell of ^{32}S. E_i = 300 MeV, E_f = 230 MeV, potential depths V = 0 and V = 19 MeV.

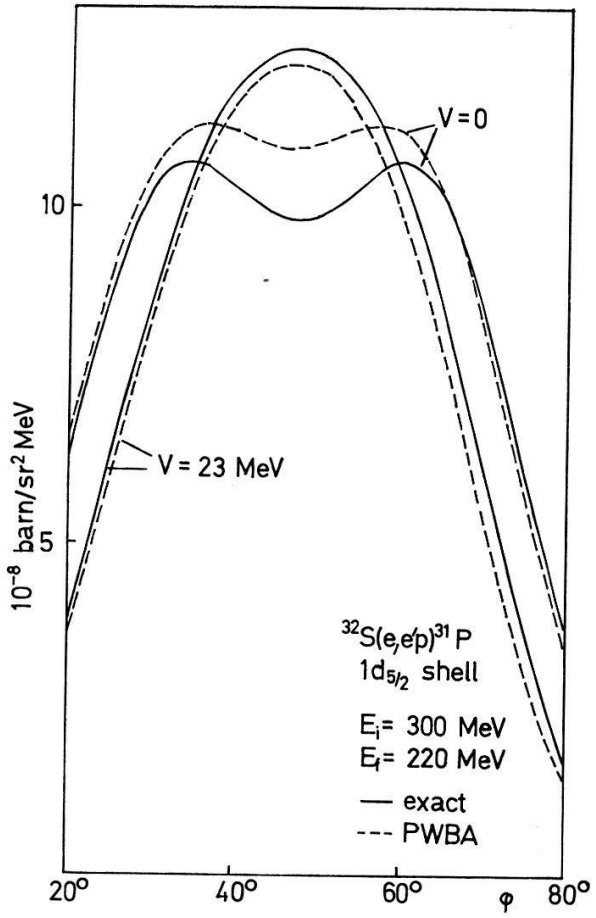

Figure 8

The coincidence cross section for the 1 $d_{5/2}$ shell of ^{32}S. E_i = 300 MeV, E_f = 220 MeV, potential depths V = 0 and V = 23 MeV.

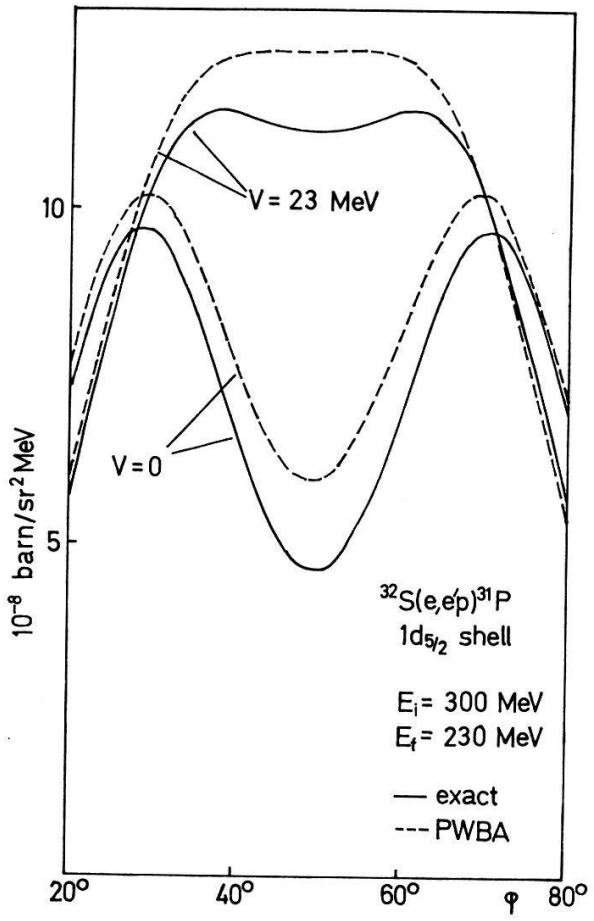

Figure 9

The coincidence cross section for the 1 $d_{5/2}$ shell of ^{32}S. E_i = 300 MeV, E_f = 230 MeV, potential depths V = 0 and V = 23 MeV.

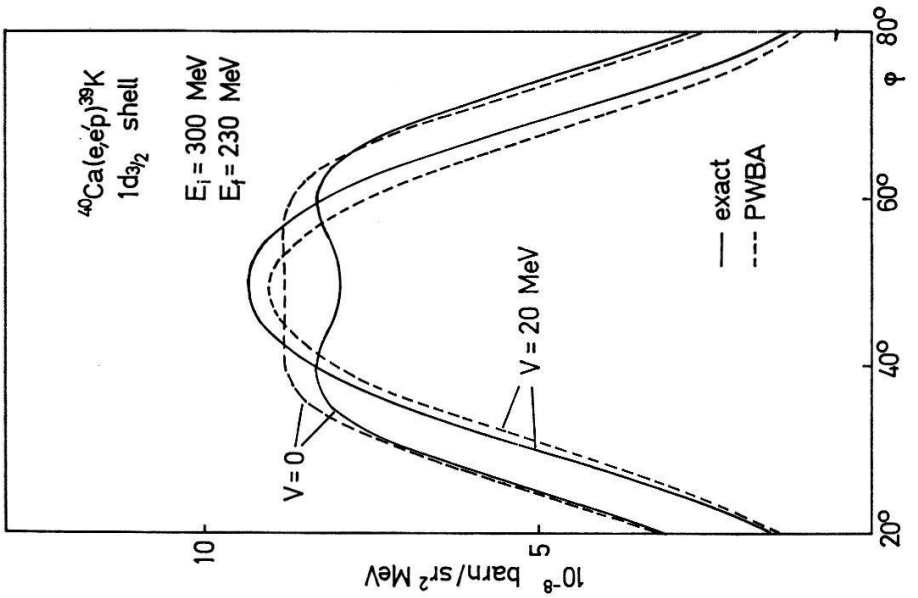

Figure 12

The coincidence cross section for the 1 $d_{3/2}$ shell of ^{40}Ca. E_i = 300 MeV, E_f = 230 MeV, potential depths $V = 0$ and $V = 20$ MeV.

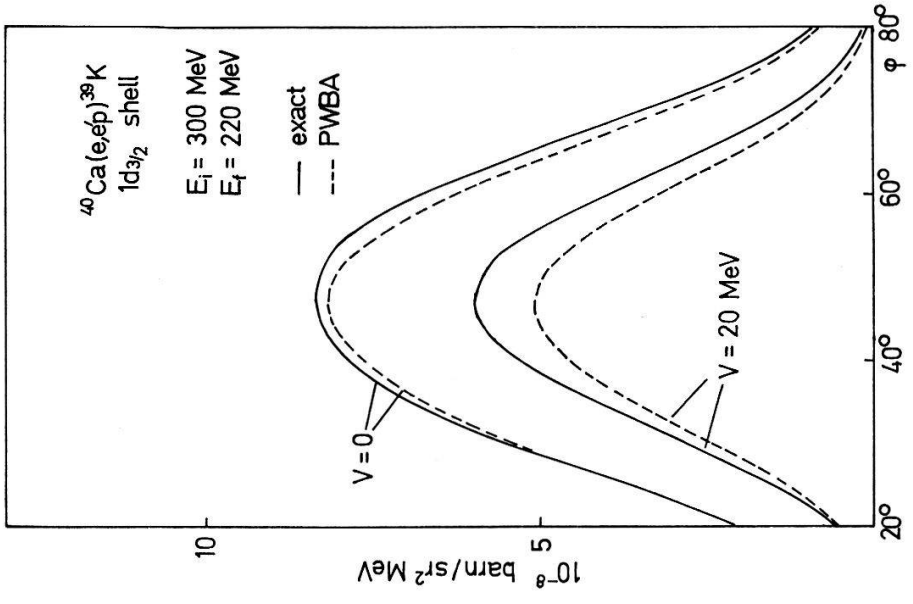

Figure 11

The coincidence cross section for the 1 $d_{3/2}$ shell of ^{40}Ca. E_i = 300 MeV, E_f = 220 MeV, potential depths $V = 0$ and $V = 20$ MeV.

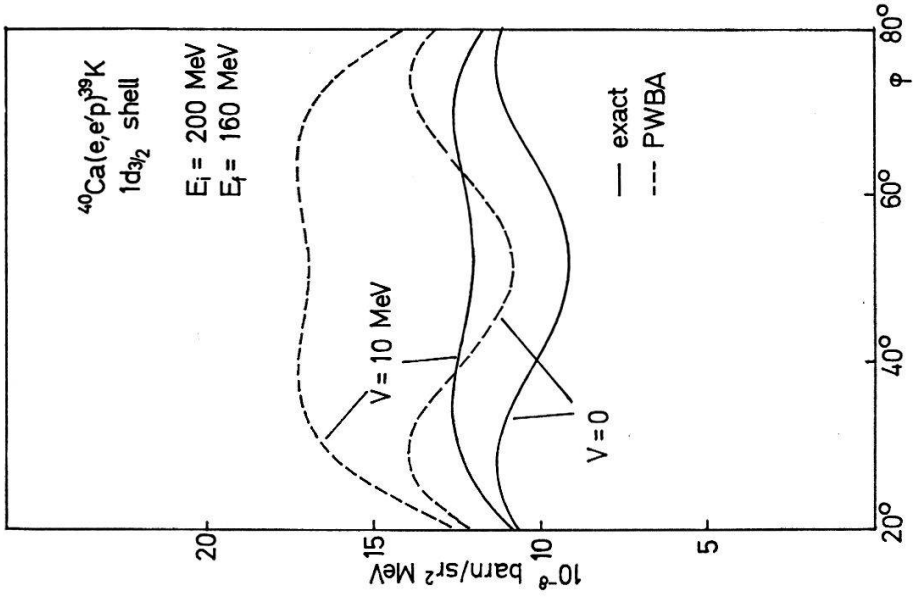

Figure 10

The coincidence cross section for the 1 $d_{3/2}$ shell of ^{40}Ca. E_i = 200 MeV, E_f = 160 MeV, potential depths $V = 0$ and $V = 10$ MeV.

Acknowledgments

The computations reported here were performed at the Computing Center of Sandoz Inc. on an UNIVAC 1108 Computer. We are indebted to Sandoz Inc. for a grant of computer time. Moreover we would like to extend our thanks to the staff of the Computing Center for their cooperation and to dipl. phys. D. Baeriswyl for his assistance with the calculations. One of us (R.V.) is grateful to the 'Schweizerischer Nationalfonds zur Förderung der Wissenschaftlichen Forschung' for support.

Appendix

A. *Harmonic Oscillator Shell Model*

The radial wave function $R_{nl}(r)$ of a particle in a harmonic oscillator shell model potential

$$V(r) = -V_0 + \frac{1}{2} m \omega^2 r^2 \tag{A.1}$$

is given by [9]

$$R_{nl}(r) = N_{nl} e^{-\frac{\lambda}{2} r^2} r^l L^{l+1/2}_{n+l+1/2}(\lambda r^2) , \tag{A.2}$$

where $L^{l+1/2}_{n+l+1/2}(\lambda r^2)$ is the Laguerre polynomial

$$L^{l+1/2}_{n+l+1/2}(\varrho) = \sum_{k=0}^{n} (-1)^k 2^k \binom{n}{k} \frac{(2l+1)!!}{(2l+2k+1)!!} \varrho^k \tag{A.3}$$

and the normalization constant N_{nl} is defined by

$$N_{nl}^2 = \frac{2^{l-n+2}(2l+2n+1)!! \lambda^{l+3/2}}{\sqrt{\pi}\, n! [(2l+1)!!]^2} . \tag{A.4}$$

The associated binding energies are given by

$$B = V_0 - (2n + l - \tfrac{1}{2})\omega . \tag{A.5}$$

The integral $\langle n l | r^2 | n l \rangle$ has the value [10]

$$\langle n l | r^2 | n l \rangle = \int_0^\infty R_{nl}^2(r)\, r^4\, dr = \frac{2n + l + 3/2}{\lambda} . \tag{A.6}$$

B. *Electron in a Central Field*

In this section, we discuss the Dirac equation for an electron in a central field. The discussion presented here is primarily to establish the notation and convention used in the text.

The solutions of the Dirac equation for an electron of energy E and mass m in a central potential $V(r)$ may be written in the form [8]

$$\psi_\varkappa^\mu = \begin{pmatrix} g_\varkappa(r)\,\chi_\varkappa^\mu \\ i\,f_\varkappa(r)\,\chi_{-\varkappa}^\mu \end{pmatrix}, \tag{B.1}$$

where the angular momentum functions are given explicitly by

$$\chi_\varkappa^\mu = \sum_\tau \langle l\, m-\tau\, \tfrac{1}{2}\,\tau \mid j\,\mu\rangle\, Y_{l\,\mu-\tau}(\hat{r}) \mid \tfrac{1}{2},\tau\rangle. \tag{B.2}$$

$\varkappa$ is the eigenvalue of the spin-orbit operator

$$(\boldsymbol{\sigma}\boldsymbol{L}+1)\,\chi_\varkappa^\mu = -\varkappa\,\chi_\varkappa^\mu \tag{B.3}$$

and is related to j and l by the following equations

$$\begin{aligned} \varkappa &= l\,(l+1) - (j+\tfrac{1}{2})^2 \\ j(\varkappa) &= |\varkappa| - \tfrac{1}{2} \\ l(\varkappa) &= j(\varkappa) + \tfrac{1}{2}\,\mathrm{sgn}\,\varkappa \quad . \end{aligned} \tag{B.4}$$

The radial functions $f_\varkappa$ and $g_\varkappa$ are solutions of the coupled differential equations

$$\frac{d}{dr}\begin{pmatrix} f_\varkappa \\ g_\varkappa \end{pmatrix} = \begin{pmatrix} \dfrac{\varkappa-1}{r} & -(E-m-V(r)) \\ E+m-V(r) & -\dfrac{\varkappa+1}{r} \end{pmatrix}\begin{pmatrix} f_\varkappa \\ g_\varkappa \end{pmatrix} \quad . \tag{B.5}$$

For the Coulomb potential $V(r) = -Z\,\alpha/r$ the regular radial wave functions are given explicitly in terms of the confluent hypergeometric function by

$$\begin{Bmatrix} f_\varkappa(r) \\ g_\varkappa(r) \end{Bmatrix} = \begin{Bmatrix} -\sqrt{\dfrac{E-m}{E+m}} \\ 1 \end{Bmatrix} (kr)^{\gamma-1}\,\frac{2^\gamma\, e^{\pi\eta/2}\,|\Gamma(\gamma+i\,\eta)|}{\Gamma(2\,\gamma+1)}$$

$$\begin{Bmatrix} Im \\ Re \end{Bmatrix} [(\gamma+i\,\eta)\, e^{i\varphi}\, e^{-ikr}\, {}_1F_1(\gamma+1+i\,\eta, 2\,\gamma+1, 2\,i\,k\,r)] \tag{B.6}$$

with

$$\begin{aligned} \gamma &= \sqrt{\varkappa^2-(\alpha\,Z)^2} \\ \eta &= \frac{\alpha\,Z\,E}{k} \\ e^{2\,i\varphi} &= \frac{-\varkappa+\dfrac{i\,\eta\,m}{E}}{\gamma+i\,\eta}\,. \end{aligned} \tag{B.7}$$

The regular Coulomb wave functions have the asymptotic forms

$$\begin{Bmatrix} f_\varkappa \\ g_\varkappa \end{Bmatrix} = \frac{1}{k\,r}\begin{Bmatrix} -\sqrt{\dfrac{E-m}{E+m}}\,\sin(k\,r+\eta\log 2\,k\,r-(l+1)\tfrac{\pi}{2}+\delta_\varkappa) \\ \cos(k\,r+\eta\log 2\,k\,r-(l+1)\tfrac{\pi}{2}+\delta_\varkappa) \end{Bmatrix} \tag{B.8}$$

where the phase shift of the partial wave is

$$\delta_\varkappa = -\arg\Gamma(\gamma+i\,\eta) + \frac{1}{2}\arg\frac{-\varkappa+\dfrac{i\,\eta\,m}{E}}{\gamma+i\,\eta} - \frac{\pi\,\gamma}{2} + (l+1)\tfrac{\pi}{2}\quad . \tag{B.9}$$

The irregular solutions are obtained from the regular solutions if γ is replaced by $-\gamma$. An incident (outgoing) electron of energy E, asymptotic momentum $\boldsymbol{k}$ and polarization τ is given by a linear combination of $\psi^{\mu}_{\varkappa}$

$$\begin{aligned}\psi_{\tau} &= 4\pi\sqrt{\frac{E+m}{2E}}\sum_{\varkappa\mu} e^{\pm i\delta_{\varkappa}}\, i^{l}\, \langle l\,\mu-\tau\,\tfrac{1}{2}\,\tau \mid j\,\mu\rangle\, Y^{*}_{l\mu-\tau}(\hat{\boldsymbol{k}})\,\psi^{\mu}_{\varkappa} \\ &= 4\pi\sqrt{\frac{E+m}{2E}}\sum_{\varkappa\mu} i^{-l}\,\hat{j}\,(-1)^{\mu-\frac{1}{2}}\begin{pmatrix} l & \frac{1}{2} & j \\ \mu-\tau & \tau & -\mu\end{pmatrix} Y^{*}_{l\mu-\tau}(\hat{\boldsymbol{k}})\, e^{\pm i\delta_{\varkappa}}\,\psi^{\mu}_{\varkappa} \qquad \text{(B.10)}\end{aligned}$$

where

$$\hat{j} = \sqrt{2j+1}\ , \quad \hat{\boldsymbol{k}} = \frac{\boldsymbol{k}}{k}\ .$$

Beyond the limits of the nuclear charge distribution the potential is simply that of a point charge, in which case the WKB method [8] can be used to obtain solutions of the form

$$\begin{cases} r\,g = \sqrt{\dfrac{E-V+m}{\sqrt{Q_0+Q_1}}}\,\exp\left(i\int\sqrt{Q_0+Q_1}\,dr\right) & \text{(B.11)} \\ r\,f = \sqrt{\dfrac{E-V-m}{\sqrt{Q_0-Q_2}}}\,\exp\left(i\int\sqrt{Q_0-Q_2}\,dr\right) & \text{(B.12)}\end{cases}$$

with

$$\begin{cases} Q_0 = E^2-m^2+\dfrac{2E\zeta}{r}-\dfrac{\gamma^2}{r^2}\ . \\ Q_1 = \dfrac{\varkappa}{r^2}\left[\dfrac{\zeta}{r(E+m)+\zeta}-1\right] \\ Q_2 = \dfrac{\varkappa}{r^2}\left[\dfrac{\zeta}{r(E-m)+\zeta}-1\right] \end{cases} \qquad \text{(B.13)}$$

$$\begin{cases} \gamma^2 = \varkappa^2-\zeta^2 \\ \zeta = Z\,\alpha \\ p^2 = E^2-m^2\ . \end{cases} \qquad \text{(B.14)}$$

With the approximation

$$\sqrt{Q_0+Q_1} \approx \sqrt{Q_0}+\frac{Q_1}{2\sqrt{Q_0}} \qquad \text{(B.15)}$$

the integral (B.11) can be evaluated explicitly giving

$$\int\left(\sqrt{Q_0}+\frac{Q_1}{2\sqrt{Q_0}}\right)dr = \sqrt{Q}+\eta\log\left(\sqrt{Q}+p\,r+\eta\right)-\gamma\,\theta+\tfrac{1}{2}\,\mathrm{sgn}\,\varkappa\,\Phi(m) \qquad \text{(B.16)}$$

with

$$\begin{cases} \theta = \arcsin \dfrac{\eta\, p\, r - \gamma^2}{\sqrt{\eta^2+\gamma^2}\, p\, r} \\ \Phi(m) = \arcsin \dfrac{-\zeta\, m\, r + \dfrac{\zeta^2}{1+\frac{m}{E}} + \gamma^2}{\left(p\, r + \dfrac{\zeta\, p}{E+m}\right)\sqrt{\eta^2+\gamma^2}} \\ Q = p^2 r^2 + 2\,\eta\, p\, r - \gamma^2 \,. \end{cases} \tag{B.17}$$

The solution of the second integral (B.12) can be found by the substitution

$$\begin{aligned} m &\to -m \\ \varkappa &\to -\varkappa \,. \end{aligned} \tag{B.18}$$

$$\int \left(\sqrt{Q_0} - \frac{Q_2}{2\sqrt{Q_0}}\right) dr = \sqrt{Q} + \eta \log(\sqrt{Q} + p\, r + \eta) - \gamma\, \theta - \tfrac{1}{2} \operatorname{sgn} \varkappa\, \Phi(-m) \quad . \tag{B.19}$$

Thus the WKB solutions with the correct asymptotic behaviour are given by

$$\begin{aligned} r\, g = \sqrt{\frac{(E+m)\, r + \zeta}{p\,(E+m)\sqrt{Q}-\varkappa}} \quad & \cos\left[(\sqrt{Q} + \eta \log(\sqrt{Q} + p\, r + \eta) - \gamma\,(\theta - \theta_0)\right. \\ & \left. + \tfrac{1}{2} \operatorname{sgn} \varkappa \left(\Phi(m) - \Phi_0(m)\right) - \eta - (l+1)\,\tfrac{\pi}{2} + \delta_\varkappa\right] \end{aligned} \tag{B.20}$$

$$\begin{aligned} r\, f = -\sqrt{\frac{(E-m)\, r + \zeta}{p\,(E+m)\sqrt{Q}+\varkappa}} \quad & \sin\left[(\sqrt{Q} + \eta \log(\sqrt{Q} + p\, r + \eta) - \gamma\,(\theta - \theta_0)\right. \\ & \left. - \tfrac{1}{2} \operatorname{sgn} \varkappa\, (\Phi(-m) + \Phi_0(m)) - \eta - (l+1)\,\tfrac{\pi}{2} + \delta_\varkappa\right] \end{aligned}$$

with the asymptotic values

$$\begin{aligned} \theta_0 &= \arcsin \frac{\eta}{\sqrt{\eta^2+\gamma^2}} \\ \Phi_0(m) &= -\,\Phi_0(-m) = \arcsin \frac{-\zeta\, m}{p\sqrt{\eta^2+\gamma^2}} \end{aligned} \tag{B.21}$$

After straight-forward calculation the angular integrals

$$\int \psi^{\mu_f}_{\varkappa_f}{}^{+}\, Y_{\lambda\mu}\, \psi^{\mu_i}_{\varkappa_i}\, d\Omega = (f_{\varkappa_i} f_{\varkappa_f} + g_{\varkappa_i} g_{\varkappa_f}) \langle \varkappa_f \mu_f \,|\, Y_{\lambda\mu} \,|\, \varkappa_i \mu_i \rangle \tag{B.22}$$

$$\begin{aligned} \int \psi^{\mu_f}_{\varkappa_f}{}^{+}\, \boldsymbol{\alpha} \cdot \boldsymbol{Y}_{\lambda\lambda-1\mu}\, \psi^{\mu_i}_{\varkappa_i}\, d\Omega = \frac{i}{\sqrt{\lambda\,(2\lambda+1)}} & \left[(\varkappa_f - \varkappa_i)\,(f_{\varkappa_f} g_{\varkappa_i} + g_{\varkappa_f} f_{\varkappa_i}) - \right. \\ & \left. \lambda\,(g_{\varkappa_f} f_{\varkappa_i} - f_{\varkappa_f} g_{\varkappa_i})\right] \langle \varkappa_f \mu_f \,|\, Y_{\lambda\mu} \,|\, \varkappa_i \mu_i \rangle \end{aligned} \tag{B.23}$$

$$\begin{aligned} \int \psi^{\mu_f}_{\varkappa_f}{}^{+}\, \boldsymbol{\alpha} \cdot \boldsymbol{Y}_{\lambda\lambda+1\mu}\, \psi^{\mu_i}_{\varkappa_i}\, d\Omega = \frac{i}{\sqrt{(\lambda+1)\,(2\lambda+1)}} & \left[(\varkappa_f - \varkappa_i)\,(f_{\varkappa_f} g_{\varkappa_i} + g_{\varkappa_f} f_{\varkappa_i})\right. \\ & \left. + (\lambda+1)\,(g_{\varkappa_f} f_{\varkappa_i} - f_{\varkappa_f} g_{\varkappa_i})\right] \langle \varkappa_f \mu_f \,|\, Y_{\lambda\mu} \,|\, \varkappa_i \mu_i \rangle \end{aligned} \tag{B.24}$$

$$\int \psi^{\mu_f}_{\varkappa_f}{}^{+} \boldsymbol{\alpha} \cdot \boldsymbol{Y}_{\lambda\lambda\mu} \psi^{\mu_i}_{\varkappa_i} d\Omega = \frac{-i}{\sqrt{\lambda(\lambda+1)}} (\varkappa_i + \varkappa_f) (f_{\varkappa_f} g_{\varkappa_i} + g_{\varkappa_f} f_{\varkappa_i})$$
$$\langle -\varkappa_f \mu_f | Y_{\lambda\mu} | \varkappa_i \mu_i \rangle \tag{B.25}$$

may be evaluated. For the integral

$$\langle \varkappa_f \mu_f | Y_{\lambda\mu} | \varkappa_i \mu_i \rangle = \int \chi^{\mu_f}_{\varkappa_f}{}^{+} Y_{\lambda\mu} \chi^{\mu_i}_{\varkappa_i} d\Omega \tag{B.26}$$

we get a contribution only for $l_f + \lambda + l_i =$ even by reason of the parity selection rule

$$\langle \varkappa_f \mu_f | Y_{\lambda\mu} | \varkappa_i \mu_i \rangle = (-1)^{\mu_f + \frac{1}{2}} \frac{\hat{j}_f \hat{\lambda} \hat{j}_i}{\sqrt{4\pi}} \begin{pmatrix} j_f & \lambda & j_i \\ -\mu_f & \mu & \mu_i \end{pmatrix} \begin{pmatrix} j_f & \lambda & j_i \\ \frac{1}{2} & 0 & -\frac{1}{2} \end{pmatrix}$$
$$\times \frac{1}{2} \left(1 + (-1)^{l_f + \lambda + l_i}\right). \tag{B.27}$$

REFERENCES

[1] G. Jacob and Th. A. J. Maris, Rev. Mod. Phys. *38*, 121 (1966).
[2] V. Devanathan, Ann. Phys. (N.Y.) *43*, 74 (1967).
[3] T. de Forest, Ann. Phys. (N.Y.) *15*, 365 (1967).
[4] G. Jacob and Th. A. J. Maris, Nucl. Phys. *31*, 139 (1962); *31*, 152 (1962).
[5] J. Potter, Nucl. Phys. *45*, 33 (1963).
[6] A. R. Edmonds, *Angular Momentum in Quantum Mechanics* (Princeton University Press, Princeton 1957).
[7] G. Källén, *Elementary Particle Physics* (Addison-Wesley Publishing Company, Inc., Reding, Massachusetts 1964).
[8] M. E. Rose, *Relativistic Electron Theory* (John Wiley & Sons, Inc., New York 1961).
[9] I. Talmi, Helv. phys. Acta *25*, 185 (1952).
[10] S. G. Nilsson, Dan. Mat. Fys. Medd. *29*, 16 (1955).
[11] D. R. Yennie, D. G. Ravenhall and R. N. Wilson, Phys. Rev. *95*, 500 (1954).
[12] U. Amaldi et al., Phys. Rev. Lett. *13*, 341 (1964).